IEEE Access
Multidisciplinary | Rapid Review | Open Access Journal

Received August 9, 2020, accepted August 16, 2020, date of publication August 24, 2020, date of current version September 4, 2020.

Digital Object Identifier 10.1109/ACCESS.2020.3019080

NOMA-Aided UAV Data Collection System: Trajectory Optimization and Communication Design

JUNWEI ZHAO, YING WANG, (Member, IEEE), ZIXUAN FEI, XUE WANG, AND ZHONGYU MIAO, (Associate Member, IEEE)

State Key Laboratory of Networking and Switching Technology, Beijing University of Posts and Telecommunications, Beijing 100876, China

Corresponding author: Ying Wang (wangying@bupt.edu.cn)

This work was supported by the Beijing Natural Science Fund-Haidian Original Innovation Joint Fund under Grant L192003.

ABSTRACT Unmanned aerial vehicle (UAV) communication has been deemed as a promising technology to collect data for the Internet of Things (IoT) in inaccessible areas. However, due to the limited UAV flight time, traditional UAV communication may not be competent for large-scale IoT data collection. This paper considers integrating non-orthogonal multiple access (NOMA) into UAV communication systems to collect data for large-scale IoT devices within UAV flight time. We aim to minimize the total energy consumption of IoT devices while ensuring data collection, by jointly optimizing UAV trajectory, IoT device scheduling and transmit power. The formulated problem is a mixed integer non-convex problem, which is challenging to solve in general. We propose a data collection optimization algorithm (DCOA) to solve it by applying the Generalized Benders Decomposition (GBD) and successive convex approximation (SCA) techniques. Then, a greedy algorithm (GA) is also proposed to reduce complexity by simplifying the optimization of UAV trajectory and IoT device scheduling. Finally, the numerical results demonstrate that, compared with traditional UAV communication systems, the NOMA-aided UAV system performs better in terms of data collection and lower total energy consumption of IoT devices can be achieved by DCOA.

INDEX TERMS Unmanned aerial vehicle (UAV) communication, non-orthogonal multiple access (NOMA), data collection, Internet of Things (IoT), energy consumption minimization.

I. INTRODUCTION

A. MOTIVATION

The Internet of Things (IoT) with powerful connection and data interaction, is promoting the development of energy, medical, agriculture and other fields, which has dramatically changed our daily life [1]–[4]. According to Cisco, 500 billion devices are expected to be connected to the Internet by 2030 [5], sensing or interacting with the internal state or the external environment and communicating over the IoT. The data collected by IoT devices (IoTDs) can be processed by IoT applications to provide insights and help make decisions and actions. However, with the expansion of the application scale, defects of IoT in data collection gradually emerge, restricting its further development.

Data collection is an essential function of IoT and the basis of IoT applications. Limited by the energy consumption, quantity and distribution of IoTDs, data collection has always been a challenge for IoT. Nowadays, the common data collection technologies are Narrow Band IoT (NB-IoT) and Long Range (LoRa), due to their advantages of wide coverage, large-scale connection and low device power consumption [6], [7]. However, both of them rely heavily on the infrastructure, such as base stations and signal towers, making them hard to catch up with the development of IoT, where more and more IoTDs are deployed in inaccessible areas, for example, in the forest to monitor the environment. It is infeasible either technically or economically to construct infrastructure in inaccessible areas. Therefore, effective data collection schemes for IoT in inaccessible areas are urgently needed.

In this context, Unmanned aerial vehicle (UAV) communication is considered as a promising technology to solve the above problem, due to its high mobility, low cost and flexible deployment [8]. UAV can be deployed flexibly in inaccessible areas at any time, significantly reducing the

The associate editor coordinating the review of this manuscript and approving it for publication was Praveen Gunturi.

cost. In addition, the line-of-sight channel between UAV and devices makes data transmission more efficient. Despite many advantages, limited flight time is still the bottleneck for UAV communication.[1] According to the data from Da-Jiang Innovations [9], the flight time of existing civil UAV is generally 10-20 minutes. Taking into account the carried communication equipment, UAV flight time will be further shortened. Thus, UAV may not be able to complete data collection in the case of the wide distribution of IoTDs. In order to finish the data collection within the flight time, it is essential to improve the efficiency of UAV communication.

Non-orthogonal multiple access (NOMA) is a powerful tool to improve spectrum efficiency and solve the access and data transmission of large-scale IoTDs [10]. Compared with orthogonal multiple access (OMA), NOMA allows simultaneous transmission of multiple users on the same frequency, relying on successive interference cancelation (SIC) techniques at the receiver. Therefore, the application of NOMA in UAV communication can effectively deal with the challenges caused by the limited UAV flight time. In this paper, we propose a NOMA-aided UAV data collection system for large-scale IoTDs in inaccessible areas. Furthermore, a data collection optimization algorithm (DCOA) is proposed to minimize the total energy consumption of IoTDs while ensuring data collection, by jointly optimizing UAV trajectory, IoTD scheduling and transmit power.

B. RELATED WORKS

1) UAV COMMUNICATION

Most of early UAV studies focused on the basic analysis of UAV communication. Al-Hourani *et al*. proposed the air to ground channel that is widely used for UAV communication [11]. Matolak *et al*. established the channel models of UAV communication in the suburbs and mountains [12], [13]. Yang *et al*. analyzed the impact of UAV trajectory and speed on flight and communication energy consumption [14]. The above studies have greatly promoted the practical application of UAV. Nowadays, researchers pay more attention to the performance of UAV communication systems. According to the optimization objective, the studies are divided into two categories, improving the performance of UAV communication systems [15]–[19] and enhancing the user performance [20]–[23]. Wu *et al*. analyzed the coverage performance of cooperative UAV clustering, revealing the optimal cooperative radius, average altitude and altitude difference in maximizing the coverage performance [15]. Khuwaja *et al*. characterized the impact of ground user mobility, propagation environment and channel fading on the outage performance of UAV communication [16]. Chakareski *et al*. designed an efficient resource management framework for enhanced coverage and throughput of UAV-based aerial small cells [17]. Energy limitation is a major bottleneck in UAV communication. Zeng *et al*. derived the propulsion power consumption model of the rotary-wing UAV and found the optimized hovering locations and durations to minimize the propulsion and communication energy of UAV [18]. In particular, Sun *et al*. proposed the solar-powered UAV, which effectively solved the limitation of UAV energy and greatly improved the stability and sustainability of UAV communication. And they maximized the system sum throughput by optimizing the 3D aerial trajectory and the wireless resource allocation [19]. In terms of enhancing user performance, Zhan *et al*. jointly optimized the wake-up schedule and UAV trajectory to minimize the maximum energy consumption of users [20]. Mozaffari *et al*. proposed a novel framework to minimize the total transmit power of devices under their SINR constraint [21]. Lin *et al*. maximized the energy efficiency of sensors by adaptively tuning the frame length at MAC layer according to UAV flying speed [22]. Wu *et al*. investigated new type of multi-UAV enabled wireless networks to maximize the minimum average rate among all users, by jointly optimizing user scheduling and association, UAV trajectory and transmit power [23]. UAV has become an indispensable part of the future communication system. It is worth noting that the above studies are based on OMA while we study the UAV communication systems with the power domain NOMA. The power domain NOMA separates the signals of multiple IoTDs at the expense of IoTD power, which leads to the coupling of IoTD scheduling and power. In addition, SIC in NOMA is generally conducted according to the descending order of the channel gain, which is affected by UAV trajectory. Therefore, the optimization of UAV trajectory, IoTD scheduling and transmit power in this paper will be much complicated.

2) NOMA

Saito *et al.* firstly presented the concept of NOMA in [24] and they investigated the system level performance of NOMA with ideal SIC in [25]. Then researchers analyzed the performance of the NOMA system in the actual communication system [26], [27]. Wang *et al*. considered the downlink of NOMA systems with statistical channel state information, deriving the ergodic data rate, the outage probability and the sum throughput of NOMA systems [26]. Ding *et al*. investigated the performance of NOMA in a cellular downlink scenario with randomly deployed users [27]. The data rate of uplink and downlink was optimized in [28] and [29]. Zhu *et al*. optimized the achievable sum rate with minimum rate constraint in a downlink 2-user NOMA network, considering user pairing and power allocation [28]. Sedagha *et al*. maximized the sum rate of single antenna multiple subcarriers NOMA uplinks under frequency-flat fading and frequency-selective fading [29]. Since the power domain NOMA is realized via different power level of users in the same frequency, the studies in [30] and [31] focused on energy efficiency of the NOMA system. Fang *et al*.

[1] The flight time of UAV is closely related to the energy consumption of UAV. As the energy consumption of UAV is affected by many factors, such as UAV load, flight speed, flight altitude, wind speed, etc., in practical, UAV flight time is more often mentioned as an important parameter of UAV. Therefore we pay more attention to UAV flight time.

aimed to maximize the system energy efficiency in a NOMA HetNet via subchannel allocation and power allocation [30]. Zeng *et al*. optimized power and sub-channel allocation to maximize the energy efficiency of multi-carrier uplink NOMA systems considering the user power restriction [31]. Pischella *et al*. paid more attention to the proportional fairness of NOMA. They proposed a graph-based clustering and resource allocation algorithm to optimize the time-based proportional fairness in the multi-carrier uplink networks [32].

Recently, some researchers considered integrating NOMA into UAV communication systems to improve UAV performance. Hou *et al*. proposed a NOMA-aided UAV network by utilizing a stochastic geometry model for providing wireless service to randomly roaming users [33]. They also proposed two connection strategies in NOMA-assisted multi-UAV communication system, user-centric strategy and UAV-centric strategy, and derived interference and coverage probability in the imperfect successive interference cancelation scenario [34]. Sohail *et al*. optimized the energy efficiency of the multi-user NOMA assisted UAV communication system by a computationally efficient method amid multi-QoS constraints [35]. Zhao *et al*. maximized the sum rate of the network served users by optimizing UAV trajectory and precoding vectors [36]. Cui *et al*. paid more attention to user fairness. They jointly optimized the trajectory design and resource allocation to maximize the minimum average rate between multiple users with the constraints of UAV flight speed and transmit power [37]. The number of users with satisfactory QoS experience was maximized in [38], by optimizing UAV deployment, admission control and power allocation. The above studies proposed some solutions to improve the performance of NOMA aided UAV communication systems. However, it is worth mention that these studies aim at the long-term benefits of the system without considering the effect of UAV flight time, which may not be applicable to the scenarios where the primary goal is to accomplish data collection of large-scale IoTDs within UAV flight time.

C. CONTRIBUTIONS AND ORGANIZATION

In this paper, we propose the NOMA-aided UAV communication system to collect data for large-scale IoTDs in inaccessible areas. The main contributions are as follows.

1) We aim to complete data collection within UAV flight time and reduce the total energy consumption of IoTDs, by jointly optimizing UAV trajectory, IoTD scheduling and transmit power, which is a challenging problem to solve due to the coupling of the variables. A data collection optimization algorithm (DCOA) is proposed to obtain a suboptimal solution.
2) The formulated problem is a mixed integer non-convex problem, which is difficult to tackle due to the coupling variables. The Generalized Benders Decomposition (GBD) is used to decouple IoTD scheduling and transmit power and get the optimal IoTD scheduling. Then, with the given IoTD scheduling, we propose a two-step iterative optimization algorithm to get the optimal UAV trajectory and IoTD transmit power by applying the successive convex approximation (SCA) technique. In addition, in order to reduce complexity, a greedy algorithm (GA) is proposed by simplifying the optimization of UAV trajectory and IoTD scheduling.
3) Numerical results show that the NOMA-aided UAV system performs better in terms of the data collection success rate of large-scale IoTDs compared with traditional UAV communication systems. Besides, numerical results also reveal that lower total energy consumption of IoTDs can be achieved by DCOA. And the greedy algorithm can greatly reduce the runtime of algorithm.

The rest of this paper is organized as follows. Section II introduces the system model and the problem formulation. In Section III, we present DCOA algorithm and GA algorithm in detail and analyze the computational complexity of these two algorithms. The numerical results are investigated in Section IV. Finally, we conclude this paper in Section V.

II. SYSTEM MODEL AND PROBLEM FOMULATION

A. SYSTEM MODEL

In this paper, as shown in Figure 1, we focus on a NOMA-aided UAV data collection system for large-scale IoTDs in inaccessible areas. IoTDs are distributed in inaccessible areas, denoted as $\mathcal{K} = \{1, 2, \ldots k, \ldots K\}$. UAV is deployed to collect data from IoTDs, denoted as u. The radius of the inaccessible areas is denoted as R.

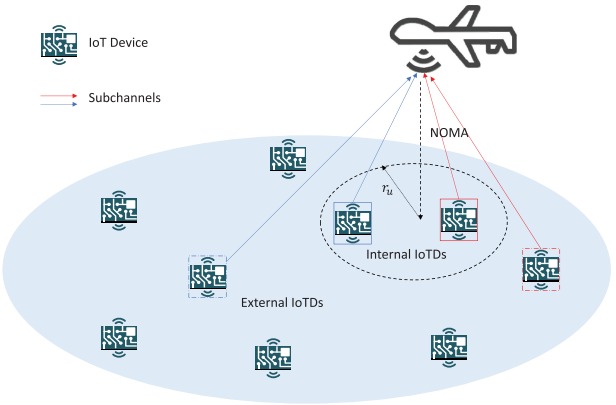

FIGURE 1. System model.

1) MODEL OF IoT DEVICES AND UAV

It is assumed that the location and data volume of IoTDs are known. The parameters of IoTD k can be expressed by the matrix $\mathbb{M}_k = \{\mathbf{D}_k, C_k, P_k, P_{max}\}$. $\mathbf{D}_k = (x_k, y_k)$ is the coordinate of IoTD. C_k is the amount of uploaded data. P_k is the transmit power, and the maximum power is denoted as P_{max}.

The parameters of UAV can be expressed by the matrix $\mathbb{M}_u = \{\mathbf{D}_u, H, V_{max}, T\}$. $\mathbf{D}_u = (x_u, y_u)$ is the horizontal coordinate of UAV. The flying height is denoted as H.

V_{max} is the maximum flight speed and T denotes the flight time. T is divided into N equal time slots, denoted as $\mathcal{N} = \{1, 2, \dots n, \dots N\}$. N is chosen large enough so that the position of UAV remains approximately unchanged in each time slot. UAV trajectory can be expressed as $\mathbf{D}_u = \{\mathbf{D}_u[1], \dots, \mathbf{D}_u[n], \dots, \mathbf{D}_u[N+1]\}$ and the following constraints need to be met.

$$\mathbf{D}_u[1] = \mathbf{D}_u[N+1], \tag{1}$$

$$\|\mathbf{D}_u[n+1] - \mathbf{D}_u[n]\|^2 \leqslant (V_{max} \cdot T_n)^2, \quad \forall n \in \mathcal{N}, \tag{2}$$

$$T_n = \frac{T}{N}. \tag{3}$$

2) CHANNEL MODEL

The UAV communication channel is divided into M subchannels, expressed as $\mathcal{M} = \{1, 2, \dots m, \dots M\}$. The subchannel bandwidth is W. Referring to [20], [23], [39], we assume that the communication channel is a line-of-sight (LOS) channel, and the channel gain follows the free space path loss model.[2] $h_k[n]$ represents the channel gain of IoTD k in time slot n. The channel gain can be assumed constant in each time slot because the position of UAV is assumed to remain approximately unchanged in each time slot in UAV model.

$$h_k[n] = \beta_0 d_{u,k}^{-2}[n] = \frac{\beta_0}{\|\mathbf{D}_u[n] - \mathbf{D}_k\|^2 + H^2}, \tag{4}$$

where β_0 represents the channel gain at the reference distance $d = 1$ m and $d_{u,k}[n]$ represents the distance between IoTD k and UAV in time slot n.

3) NOMA MODEL

As shown in Figure 1, we divide IoTDs into two sets $\mathcal{K}_I$ and $\mathcal{K}_O$ by a circle with the horizontal position of UAV as the center and r_u as the radius. $\mathcal{K}_I = \{\mathcal{K}_I[1], \dots, \mathcal{K}_I[N]\}$. $\mathcal{K}_O = \{\mathcal{K}_O[1], \dots, \mathcal{K}_O[N]\}$. In time slot n, if an IoTD is in the circle, it is called internal IoTD and belongs to $\mathcal{K}_I[n]$. Otherwise, the IoTD is called external IoTD and belongs to $\mathcal{K}_O[n]$. $\mathcal{K} = \mathcal{K}_I[n] \cup \mathcal{K}_O[n]$. $\mathcal{K}_I[n] \cap \mathcal{K}_O[n] = \emptyset$, $\forall n \in \mathcal{N}$. We assume that only one internal IoTD and one external IoTD are allowed at channel m in time slot n.

Referring to [24] and [25], SIC is conducted according to the descending order of channel gain at the receiver. Since the channel gain of external IoTD is less than the channel gain of internal IoTD, the signal-to-interference and noise ratio of IoTD k can be expressed as

$$\gamma_k[n][m] = \begin{cases} \dfrac{P_k[n]h_k[n]}{I_k[n][m] + \sigma^2} & if\ k \in \mathcal{K}_I[n], \\ \dfrac{P_k[n]h_k[n]}{\sigma^2} & if\ k \in \mathcal{K}_O[n], \end{cases} \quad \forall n \in \mathcal{N}, \quad \forall m \in \mathcal{M}, \tag{5}$$

where σ^2 represents the power spectral density of noise. $I_k[n][m]$ is the interference from external IoTD that access the same channel m with internal IoTD k in time slot n.

[2]UAV flies at a higher altitude and there are few buildings in inaccessible areas, so there are almost no obstructions between UAV and IoTDs. Therefore the LOS channel can be used as the air-to-ground link channel model. The channel gain follows the free space path loss model.

IoTD scheduling is expressed as $\alpha_k[n][m]$. If IoTD k is served by UAV at channel m in time slot n, $\alpha_k[n][m] = 1$. Otherwise, $\alpha_k[n][m] = 0$. Therefore, the achievable rate of IoTD k can be denoted as

$$R_k^I[n][m] = W\log_2\left(1 + \frac{\alpha_k[n][m]P_k[n]h_k[n]}{\sum\limits_{i \in \mathcal{K}_O[n]} \alpha_i[n][m]P_i[n]h_i[n] + \sigma^2}\right), \quad \forall k \in \mathcal{K}_I[n], \quad \forall n \in \mathcal{N}, \ \forall m \in \mathcal{M}. \tag{6}$$

$$R_k^O[n][m] = W\log_2\left(1 + \frac{\alpha_k[n][m]P_k[n]h_k[n]}{\sigma^2}\right), \quad \forall k \in \mathcal{K}_O[n], \quad \forall n \in \mathcal{N}, \ \forall m \in \mathcal{M}. \tag{7}$$

B. PROBLEM FORMULATION

The optimization goal of this paper is to accomplish data collection and minimize the total energy consumption E of IoTDs by optimizing UAV trajectory $\mathbf{D}_u[n]$, IoTD scheduling $\alpha_k[n][m]$ and IoTD transmit power $P_k[n]$.

$$E = T_n \cdot \sum_{n=1}^{N}\sum_{k=1}^{K}\sum_{m=1}^{M} \alpha_k[n][m]P_k[n]. \tag{8}$$

The trajectory optimization and communication design problem of the NOMA-aided UAV data collection system can be formulated as

$$P: \min_{\mathbf{D}_u[n], \alpha_k[n][m], P_k[n]} \quad E$$

$$s.t.\ 0 \leqslant P_k[n] \leqslant P_{max}, \quad \forall k \in \mathcal{K}, \ \forall n \in \mathcal{N}, \tag{9a}$$

$$T_n \cdot \sum_{n=1}^{N}\sum_{m=1}^{M}\left(R_k^I[n][m] + R_k^O[n][m]\right) \geqslant C_k, \quad \forall k \in \mathcal{K}, \tag{9b}$$

$$\sum_{i \in \mathcal{K}_I[n]} \alpha_i[n][m] + \sum_{j \in \mathcal{K}_O[n]} \alpha_j[n][m] \leqslant 2, \quad \forall n \in \mathcal{N}, \forall m \in \mathcal{M}, \tag{9c}$$

$$\sum_{m=1}^{M} \alpha_k[n][m] \leqslant 1, \quad \forall k \in \mathcal{K}, \ \forall n \in \mathcal{N}, \tag{9d}$$

$$\alpha_k[n][m] = \{0, 1\}, \quad \forall k \in \mathcal{K}, \quad \forall n \in \mathcal{N}, \quad \forall m \in \mathcal{M}, \tag{9e}$$

$$\|\mathbf{D}_u[n+1] - \mathbf{D}_u[n]\|^2 \leqslant (V_{max} \cdot T_n)^2, \quad \forall n \in \mathcal{N}, \tag{9f}$$

$$\mathbf{D}_u[1] = \mathbf{D}_u[N+1], \tag{9g}$$

where (9a) is IoTD transmit power constraint. (9b) indicates that the data collection needs to be accomplished within UAV flight time. (9c) ensures that only one internal IoTD and one external IoTD are allowed at any subchannel in any time slot. (9d) implies that IoTD can only access one subchannel in any time slot. (9f) and (9g) are UAV trajectory constraints.

For problem **P**, the variables $\alpha_k[n][m]$ are binary, and $\alpha_k[n][m]$, $P_k[n]$ and $\mathbf{D}_u[n]$ are coupled in (9b). So problem **P** is a mixed integer non-convex problem. In addition, $\mathcal{K}_I$ and $\mathcal{K}_O$ are determined by the position of UAV, which cannot be presented by formula. Thus solving problem **P** optimally is challenging in general.

III. PROPOSED ALGORITHM

Notation: For variable A, A^* represents the optimal value. $\tilde{A}$, $\bar{A}$ or $\hat{A}$ represent the feasible value.

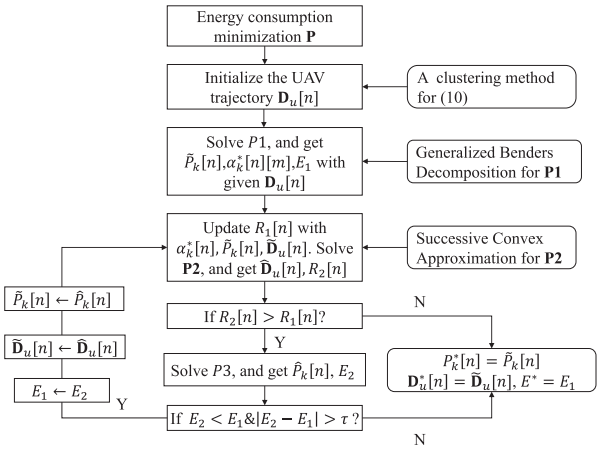

FIGURE 2. The block diagram of DCOA.

In this section, we discuss the proposed DCOA algorithm for solving problem **P**. The block diagram of DCOA is illustrated in Figure 2. We first initialize UAV trajectory $\mathbf{D}_u[n]$ with a clustering method. Then, Generalized Benders Decomposition is used to get the optimal IoTD scheduling $\alpha_k^*[n][m]$ with given $\mathbf{D}_u[n]$. Next, we formulate problem **P2** with the goal of maximizing the amount of uploaded data and problem **P3** with the goal of minimizing the total energy consumption of IoTDs. Finally, UAV trajectory and transmit power are optimized by iteratively solving **P2** and **P3** under the condition that the amount of uploaded data is increased and the total energy consumption is reduced.

A. UAV TRAJECTORY INITIALIZATION

UAV trajectory is initialized based on the position and the uploaded data of IoTDs. Specifically, the initial UAV trajectory is designed as a circle. The center is expressed as

$$(x_0, y_0) = \sum_{k=1}^{K} \varpi_k (x_k, y_k), \tag{10}$$

where $\varpi_k = C_k \Big/ \sum_{k=1}^{K} C_k$. The radius is denoted by

$$R_u = \varsigma \frac{T \cdot V_{max}}{2\pi}, \tag{11}$$

where $\varsigma (0 < \varsigma < 1)$ is the parameter to regulate UAV trajectory. Thus, the initial position of UAV in time slot n can be expressed as

$$\mathbf{D}_u[n] = \begin{cases} x[n] = x_0 + R_u \cos \dfrac{(n-1)\cdot 2\pi}{N}, \\ y[n] = y_0 + R_u \sin \dfrac{(n-1)\cdot 2\pi}{N}. \end{cases} \tag{12}$$

Therefore, radius r_u of the internal IoTD area is denoted as

$$r_u = \frac{\|\mathbf{D}_u[n] - \mathbf{D}_u[n-1]\|}{2}. \tag{13}$$

B. IoTD SCHEDULING OPTIMIZATION

With given $\mathbf{D}_u[n]$ and r_u, IoTD scheduling and transmit power can be optimized by solving problem **P1**.

$$\begin{aligned} P1: \min_{\alpha_k[n][m], P_k[n]} \; & T_n \cdot \sum_{n=1}^{N}\sum_{k=1}^{K}\sum_{m=1}^{M} \alpha_k[n][m] P_k[n] \\ s.t.\; & 0 \leqslant P_k[n] \leqslant P_{max}, \; \forall k \in \mathcal{K}, \; \forall n \in \mathcal{N}, \quad (14a) \\ & T_n \cdot \sum_{n=1}^{N}\sum_{m=1}^{M} \left(R_k^I[n][m] + R_k^O[n][m] \right) \geqslant C_k, \\ & \qquad \forall k \in \mathcal{K}, \quad (14b) \\ & \sum_{i \in \mathcal{K}_I[n]} \alpha_i[n][m] + \sum_{j \in \mathcal{K}_O[n]} \alpha_j[n][m] \leqslant 2, \\ & \qquad \forall n \in \mathcal{N}, \forall m \in \mathcal{M}, \quad (14c) \\ & \sum_{m=1}^{M} \alpha_k[n][m] \leqslant 1, \; \forall k \in \mathcal{K}, \; \forall n \in \mathcal{N}, \quad (14d) \\ & \alpha_k[n][m] = \{0, 1\}, \quad \forall k \in \mathcal{K}, \; \forall n \in \mathcal{N}, \\ & \qquad \forall m \in \mathcal{M}. \quad (14e) \end{aligned}$$

P1 is a mixed integer nonlinear programming problem (MINLP). We intend to solve this problem with Generalized Benders Decomposition [40], [41]. **P1** can be decomposed into two sub-problems, the primal problem with only continuous variables $P_k[n]$ and the master problem with only integer variables $\alpha_k[n][m]$. By iteratively solving these two sub-problems, the optimal solution is obtained. Specifically, in the v-th iteration of GBD, the upper bound of problem **P1** can be updated by solving the primal problem, and optimality cut or feasibility cut can be obtained as the constraints of master problem. By solving the master problem, the lower bound of problem **P1** can be updated, and the optimal $\alpha_k^{(v)}[n][m]$ can be obtained for the primal problem of the next iteration. When the difference between the upper bound and lower bound is less than the threshold δ, the iteration converges.

1) SOLVING THE PRIMAL PROBLEM

In the v-th iteration of GBD, with given integer variable $\alpha_k^{(v)}[n][m]$, the primal problem can be expressed as

$$\begin{aligned} \min_{P_k[n]} \; & T_n \cdot \sum_{n=1}^{N}\sum_{k=1}^{K}\sum_{m=1}^{M} \alpha_k^{(v)}[n][m] P_k[n] \\ s.t.\; & 0 \leqslant P_k[n] \leqslant P_{max}, \quad \forall k \in \mathcal{K}, \; \forall n \in \mathcal{N}, \quad (15a) \\ & T_n \cdot \sum_{n=1}^{N}\sum_{m=1}^{M} \left(R_k^I[n][m] + R_k^O[n][m] \right) \geqslant C_k, \quad \forall k \in \mathcal{K}. \\ & \qquad (15b) \end{aligned}$$

(15) is a non-convex problem due to the non-convex constraint (15b). We apply dual decomposition and SCA to relax (15) into a convex problem.

Dual Decomposition: With the Lagrange dual, the Lagrange function of (15) can be denoted as

$$\begin{aligned}&\mathfrak{L}(P_k[n],\boldsymbol{\eta})\\&=T_n\cdot\sum_{n=1}^{N}\sum_{k=1}^{K}\sum_{m=1}^{M}\alpha_k^{(v)}[n][m]P_k[n]\\&\quad+\sum_{k=1}^{K}\eta_k\left(C_k-T_n\cdot\sum_{n=1}^{N}\sum_{m=1}^{M}\left(R_k^I[n][m]+R_k^O[n][m]\right)\right),\end{aligned}\tag{16}$$

where $\boldsymbol{\eta}=[\eta_1,\ldots,\eta_k,\ldots,\eta_K]^T$, $\eta_k\geqslant 0$ is the Lagrange multiplier vector. Problem (15) can be written as

$$\min_{0\leqslant P_k[n]\leqslant P_{max}}\ \max_{\eta_k\geqslant 0}\ \mathfrak{L}(P_k[n],\boldsymbol{\eta}).\tag{17}$$

The dual problem can be expressed as

$$\max_{\eta_k\geqslant 0}\ \min_{0\leqslant P_k[n]\leqslant P_{max}}\ \mathfrak{L}(P_k[n],\boldsymbol{\eta}).\tag{18}$$

(18) can be decomposed into a two-layer optimization problem, the inner layer minimization problem with variable $P_k[n]$ and the outer layer maximization problem with variable $\boldsymbol{\eta}$. By iteratively solving these two problems, the optimal solution of problem (18) is obtained.

a: INNER LAYER MINIMIZATION

In the u-th iteration, with given $\boldsymbol{\eta}^{(u)}$, the inner layer minimization problem is expressed as

$$\min_{0\leqslant P_k[n]\leqslant P_{max}}\ \mathfrak{L}(P_k[n],\boldsymbol{\eta}^{(u)}),\tag{19}$$

where

$$\mathfrak{L}(P_k[n],\boldsymbol{\eta}^{(u)})=\sum_{k=1}^{K}\eta_k^{(u)}C_k+\sum_{n=1}^{N}\sum_{k=1}^{K}\sum_{m=1}^{M}(\mathfrak{L}_1+\mathfrak{L}_2),\tag{20}$$

$$\mathfrak{L}_1=T_n\cdot\alpha_k^{(v)}[n][m]P_k[n]-T_n\cdot\eta_k^{(u)}R_k^O[n][m],\tag{21}$$

$$\mathfrak{L}_2=-T_n\cdot\eta_k^{(u)}R_k^I[n][m].\tag{22}$$

Since $R_k^I[n][m]$ is a non-concave function with respect to $P_k[n]$, (19) is not a convex minimization problem. Referring to [23], we get the sub-optimal solution of problem (19) by relaxing $R_k^I[n][m]$ with SCA.

$R_k^I[n][m]$ can be written as the difference of two concave functions $\bar{R}_k^I[n][m]$ and $\hat{R}_k^I[n][m]$.

$$\begin{aligned}&R_k^I[n][m]\\&=W\log_2\left(1+\frac{\alpha_k^{(v)}[n][m]P_k[n]h_k[n]}{\sum\limits_{i\in\mathcal{K}_O[n]}\alpha_i^{(v)}[n][m]P_i[n]h_i[n]+\sigma^2}\right)\\&=\bar{R}_k^I[n][m]-\hat{R}_k^I[n][m],\end{aligned}\tag{23}$$

where

$$\bar{R}_k^I[n][m]=W\log_2\left(\sum_{i\in\mathcal{K}_O[n]}\alpha_i^{(v)}[n][m]P_i[n]h_i[n]+\sigma^2\right),\tag{24}$$

$$\hat{R}_k^I[n][m]=W\log_2\left(\sum_{i\in\mathcal{K}_O[n]}\alpha_i^{(v)}[n][m]P_i[n]h_i[n]+\sigma^2\right).\tag{25}$$

In order to tackle the non-concave function [25], in the r-th iteration of SCA, we perform the first-order Taylor expansion of $\hat{R}_k^I[n][m]$ at $P_i^{(r)}[n]$, and approximate $\hat{R}_k^I[n][m]$ as a linear function $\hat{R}_k^{I(ub)}[n][m]$.

$$\begin{aligned}&\hat{R}_k^I[n][m]\\&=W\log_2\left(\sum_{i\in\mathcal{K}_O[n]}\alpha_i^{(v)}[n][m]P_i[n]h_i[n]+\sigma^2\right)\\&\leqslant W\cdot\left(\begin{array}{l}\sum\limits_{i\in\mathcal{K}_O[n]}A_i[n][m]\left(P_i[n]-P_i^{(r)}[n]\right)\\+\log_2\left(\sum\limits_{i\in\mathcal{K}_O[n]}\alpha_i^{(v)}[n][m]P_i^{(r)}[n]h_i[n]+\sigma^2\right)\end{array}\right)\\&\triangleq\hat{R}_k^{I(ub)}[n][m],\end{aligned}\tag{26}$$

$$A_i[n][m]=\frac{\log_2(e)\cdot\alpha_i^{(v)}[n][m]h_i[n]}{\sum\limits_{i\in\mathcal{K}_O[n]}\alpha_i^{(v)}[n][m]P_i^{(r)}[n]h_i[n]+\sigma^2}.\tag{27}$$

Then (22) can be transformed into the following convex function.

$$\hat{\mathfrak{L}}_2=-T_n\cdot\eta_k^{(u)}\left(\bar{R}_k^I[n][m]-\hat{R}_k^{I(ub)}[n][m]\right).\tag{28}$$

The key to the transformation is that $\hat{R}_k^I[n][m]$ is a concave function with respect to $P_k[n]$. According to [42], the first-order Taylor expansion of the concave function at any point is the global upper bound of the function. Therefore, $\hat{R}_k^I[n][m]\leqslant\hat{R}_k^{I(ub)}[n][m]$ and $\mathfrak{L}_2\leqslant\hat{\mathfrak{L}}_2$. Thus, the transformation will not expand the range of problem (19).

Thus, the inner layer minimization problem (19) can be rewritten as

$$\begin{aligned}&\min_{0\leqslant P_k[n]\leqslant P_{max}}\ \hat{\mathfrak{L}}(P_k[n],\boldsymbol{\eta}^{(u)})\\&\qquad=\sum_{k=1}^{K}\eta_k^{(u)}C_k+\sum_{n=1}^{N}\sum_{k=1}^{K}\sum_{m=1}^{M}\left(\mathfrak{L}_1+\hat{\mathfrak{L}}_2\right).\end{aligned}\tag{29}$$

It can be found that the first derivative of the function $\hat{\mathfrak{L}}(P_k[n],\boldsymbol{\eta}^{(u)})$ with respect to $P_k[n]$ is an increasing function, so the optimal solution of (29) can be denoted as

$$\tilde{P}_k[n]=\begin{cases}0 & \bar{P}_k[n]<0\\ \bar{P}_k[n] & 0\leqslant\bar{P}_k[n]\leqslant P_{max}\\ P_{max} & \bar{P}_k[n]>P_{max}.\end{cases}\tag{30}$$

$$\frac{\partial\hat{\mathfrak{L}}(\bar{P}_k[n],\boldsymbol{\eta}^{(u)})}{\partial P_k[n]}=0.\tag{31}$$

The SCA algorithm for problem (19) is shown in **Algorithm** 1.

Algorithm 1 Successive Convex Approximation Algorithm for Solving the Inner Minimization Problem (19)

Input: Objective function $\mathfrak{L}(P_k[n], \boldsymbol{\eta}^{(u)})$, the threshold ε.
Output: $\tilde{P}_k^{(u)}[n]$.

1: Set $r = 1$. Choose arbitrary $P_k^{(1)}[n]$ in the feasible set.
2: Calculate $\hat{\mathfrak{L}}^{(1)}(P_k^{(1)}[n], \boldsymbol{\eta}^{(u)})$.
3: **repeat**
4: Solve (29) with given $P_k^{(r)}[n]$, and get $\tilde{P}_k[n]$ according to (30).
5: $r \leftarrow r+1$, $P_k^{(r)}[n] \leftarrow \tilde{P}_k[n]$.
6: Calculate $\hat{\mathfrak{L}}^{(r)}(P_k^{(r)}[n], \boldsymbol{\eta}^{(u)})$.
7: **until** $\left|\hat{\mathfrak{L}}^{(r+1)} - \hat{\mathfrak{L}}^{(r)}\right| \leqslant \varepsilon$.
8: $\tilde{P}_k^{(u)}[n] = P_k^{(r)}[n]$.

b: OUTER LAYER MAXIMIZATION

In the u-th iteration, $\tilde{P}_k^{(u)}[n]$ is the optimal solution of the inner layer minimization problem (19). With given $\tilde{P}_k^{(u)}[n]$, the outer layer maximization problem is expressed as

$$\max_{\eta_k \geqslant 0} \mathfrak{L}(\boldsymbol{\eta}, \tilde{P}_k^{(u)}[n]). \tag{32}$$

Since $\mathfrak{L}(\boldsymbol{\eta}, \tilde{P}_k^{(u)}[n])$ is differentiable with respect to η_k, the gradient method can be applied to solve the multiplier $\eta_k^{(u+1)}$.

$$\eta_k^{(u+1)} = \left[\eta_k^{(u)} + \varphi \frac{\partial \mathfrak{L}\left(\eta_k, \tilde{P}_k^{(u)}[n]\right)}{\partial \eta_k}\right]^+, \tag{33}$$

where $\varphi(\varphi > 0)$ is the step size in the u-th iteration. The iteration terminates when $\left|\mathfrak{L}^{(u+1)} - \mathfrak{L}^{(u)}\right| \leqslant \kappa$, where κ is the threshold.

Hence, the optimal solution of the primal problem in the v-th iteration of GBD can be obtained by solving problem (19) and (32). $\tilde{P}_k^{(v)}[n] = \tilde{P}_k^{(u)}[n]$ and $\tilde{\boldsymbol{\eta}}^{(v)} = \tilde{\boldsymbol{\eta}}^{(u)}$.

The Algorithm 2 for the primal problem is as follows.

Algorithm 2 A Two-Layer Iteration Optimization Algorithm for Solving the Primal Problem

Input: $\alpha_k^{(v)}[n][m]$, objective function $\mathfrak{L}(P_k[n], \boldsymbol{\eta})$, P_{max}, κ.
Output: $\tilde{P}_k^{(v)}[n]$, $\tilde{\boldsymbol{\eta}}^{(v)}$.

1: Set $u = 1$. Choose arbitrary $\boldsymbol{\eta}^{(1)}$ in the feasible set.
2: **repeat**
3: Solve (19) with given $\boldsymbol{\eta}^{(u)}$ by **Algorithm 1**, and get $\tilde{P}_k^{(u)}[n]$.
4: Calculate $\mathfrak{L}^{(u)}(\tilde{P}_k^{(u)}[n], \boldsymbol{\eta}^{(u)})$.
5: Solve (32) with given $\tilde{P}_k^{(u)}[n]$, and calculate $\boldsymbol{\eta}^{(u+1)}$ according to (33).
6: $u \leftarrow u+1$.
7: **until** $\left|\mathfrak{L}^{(u+1)} - \mathfrak{L}^{(u)}\right| \leqslant \kappa$.
8: $\tilde{P}_k^{(v)}[n] = \tilde{P}_k^{(u)}[n]$, $\tilde{\boldsymbol{\eta}}^{(v)} = \tilde{\boldsymbol{\eta}}^{(u)}$.

2) FEASIBILITY CHECK FOR THE PRIMAL PROBLEM

In the v-th iteration of GBD, $\alpha_k^{(v)}[n][m]$ for the primal problem is the optimal solution of the master problem in the $(v-1)$-th iteration. However, not all $\alpha_k^{(v)}[n][m]$ make the primal problem feasible. Therefore, with given $\alpha_k^{(v)}[n][m]$, there are two cases for the primal problem, feasibility and infeasibility.

a: THE PRIMAL PROBLEM IS FEASIBLE

If the primal problem is feasible in the v-th iteration, we can get the optimality cut and add it as a constraint of the master problem.

$$\mathfrak{L}(\alpha_k[n][m], \tilde{P}_k^{(v)}[n], \quad \tilde{\boldsymbol{\eta}}^{(v)}) \leqslant \theta. \tag{34}$$

b: THE PRIMAL PROBLEM IS INFEASIBLE

If the primal problem is infeasible, define a set of $\tilde{\boldsymbol{\eta}}^{(v)} \in \Lambda = \left\{\eta_k \geqslant 0 \middle| \sum_{k=1}^{K} \eta_k = 1\right\}$ which should satisfy

$$\min_{0 \leqslant P_k[n] \leqslant P_{max}} \bar{\mathfrak{L}}(\alpha_k^{(v)}[n][m], P_k[n], \quad \tilde{\boldsymbol{\eta}}^{(v)}) > 0, \tag{35}$$

where

$$\bar{\mathfrak{L}} = \sum_{k=1}^{K} \tilde{\eta}_k^{(v)} \begin{pmatrix} C_k \\ -T_n \cdot \sum_{n=1}^{N} \sum_{m=1}^{M} \left(R_k^I[n][m] + R_k^O[n][m]\right) \end{pmatrix}. \tag{36}$$

The calculation of $\tilde{\boldsymbol{\eta}}^{(v)}$ is presented in APPENDIX A. By solving (35), the optimal $\tilde{P}_k^{(v)}[n]$ is obtained. The feasibility cut can be denoted as

$$\bar{\mathfrak{L}}(\alpha_k[n][m], \tilde{P}_k^{(v)}[n], \quad \tilde{\boldsymbol{\eta}}^{(v)}) \leqslant 0. \tag{37}$$

3) SOLVING THE MASTER PROBLEM

With the given optimality cut and feasibility cut, the master problem can be expressed as

$$\min_{\alpha_k[n][m], \theta} \quad \theta$$

$$s.t.\ \mathfrak{L}(\alpha_k[n][m], \tilde{P}_k^{(u)}[n], \tilde{\eta}_k^{(u)}) \leqslant \theta, \quad \forall u \in \{1, 2, \ldots v_1\}, \tag{38a}$$

$$\bar{\mathfrak{L}}(\alpha_k[n][m], \tilde{P}_k^{(w)}[n], \tilde{\eta}_k^{(w)}) \leqslant 0, \quad \forall w \in \{1, 2, \ldots v_2\}, \tag{38b}$$

$$\sum_{i \in \mathcal{K}_I[n]} \alpha_i[n][m] + \sum_{j \in \mathcal{K}_O[n]} \alpha_j[n][m] \leqslant 2, \quad \forall n \in \mathcal{N}, \quad \forall m \in \mathcal{M}, \tag{38c}$$

$$\sum_{m=1}^{M} \alpha_k[n][m] \leqslant 1, \quad \forall k \in \mathcal{K}, \quad \forall n \in \mathcal{N}, \tag{38d}$$

$$\alpha_k[n][m] = \{0, 1\}, \quad \forall k \in \mathcal{K}, \quad \forall n \in \mathcal{N}, \quad \forall m \in \mathcal{M}, \tag{38e}$$

where v_1 is the number of times the primal problem is feasible, and v_2 is the number of times the primal problem is infeasible. $v_1 + v_2 = v$. Problem (38) is a 0-1 integer

programming problem, which can be solved by the branch and bound method or the cut plane method [43], [44].

With the dual decomposition and the first-order Taylor expansion, the primal problem is transformed into a convex optimization problem. Therefore, according to [45], the convergence of GBD algorithm can be guaranteed. In addition, it should be noted that the primal problem must be feasible in the first iteration of GBD algorithm [41].

GBD algorithm for problem **P1** is shown in **Algorithm** 3.

Algorithm 3 Generalized Benders Decomposition for Solving **P1**

Input: $N, M, K, C_k, \mathbf{D}_k, P_{max}, \mathbf{D}_u[n], T, \mathcal{K}_I[n], \mathcal{K}_O[n]$.
Output: $\alpha_k^*[n][m], \tilde{P}_k[n]$.

1: **Initialization:** the iteration index $v = 1$, $\mathrm{LB}(0) = 0$, $\mathrm{UB}(0) = 2T_n \cdot MN \cdot P_{max}$, $\alpha_k^{(1)}[n][m]$ in the feasible set, the threshold ε, and the maximum number of iteration v_{max}.
2: **repeat**
3: Solve the primal problem (15) with given $\alpha_k^{(v)}[n][m]$ by **Algorithm 2**.
4: **if** (15) is feasible **then**
5: Get the optimal transmit power $\tilde{P}_k^{(v)}[n]$, $\tilde{\boldsymbol{\eta}}^{(v)}$ and the optimal objective value $\tilde{E}$.
6: Obtain the optimality cut with dual decomposition.
7: The upper bound value is updated with $\mathrm{UB}(v) = \min\left\{\mathrm{UB}(v-1), \tilde{E}\right\}$.
8: **else**
9: Solve problem (35) and get $\tilde{P}_k^{(v)}[n]$, $\tilde{\boldsymbol{\eta}}^{(v)}$.
10: Obtain the feasibility cut according to (37).
11: **end if**
12: Add the optimality cut or the feasibility cut to the master problem.
13: Solve the master problem (38) with branch and bound method, and get $\alpha_k^{(v)}[n][m]$. Update $\mathrm{LB}(v)$.
14: **if** $|\mathrm{UB}(v) - \mathrm{LB}(v)| \leqslant \varepsilon$ **then**
15: Global optimal solution = **true**;
16: **return** $\tilde{P}_k[n] = \tilde{P}_k^{(v)}[n]$, $\alpha_k^*[n][m] = \alpha_k^{(v)}[n][m]$.
17: **else**
18: $v \leftarrow v + 1$.
19: **end if**
20: **until** Convergence = **true** or $v = v_{max}$.

C. UAV TRAJECTORY OPTIMIZATION

With given $\alpha_k^*[n][m]$ and $\tilde{P}_k[n]$, in this subsection, we maximize the amount of uploaded data per time slot to optimize UAV trajectory.

$$P2: \max_{\mathbf{D}_u[n],\rho[n]} \ \rho[n]$$
$$s.t.\ T_n \cdot \sum_{k=1}^{K}\sum_{m=1}^{M}\left(R_k^I[n][m] + R_k^O[n][m]\right) \geqslant \rho[n], \quad \forall n \in \mathcal{N}, \quad (39a)$$
$$\|\mathbf{D}_u[n+1] - \mathbf{D}_u[n]\|^2 \leqslant (V_{max} \cdot T_n)^2, \quad \forall n \in \mathcal{N}, \quad (39b)$$
$$\|\mathbf{D}_u[n] - \mathbf{D}_u[n-1]\|^2 \leqslant (V_{max} \cdot T_n)^2, \quad \forall n \in \mathcal{N}, \quad (39c)$$
$$\mathbf{D}_u[1] = \mathbf{D}_u[N+1]. \quad (39d)$$

(39b) and (39c) are convex sets, because UAV trajectory in other time slots is available when optimizing UAV trajectory in time slot n. (39a) is a non-convex constraint, so (39) is not a concave maximization problem, which cannot be solved directly in general.

$R_k^I[n][m]$ in (39a) can be expressed as

$$R_k^I[n][m] = W\log_2\left(1 + \frac{\frac{\alpha_k[n][m]\tilde{P}_k[n]\beta_0}{\|\mathbf{D}_u[n]-\mathbf{D}_k\|^2+H^2}}{\sum\limits_{i\in\mathcal{K}_O[n]}\frac{\alpha_i[n][m]\tilde{P}_i[n]\beta_0}{\|\mathbf{D}_u[n]-\mathbf{D}_i\|^2+H^2} + \sigma^2}\right) = \bar{R}_k^I[n][m] - \hat{R}_k^I[n][m], \quad (40)$$

where

$$\bar{R}_k^I[n][m] = W\log_2\left(\frac{\frac{\alpha_k[n][m]\tilde{P}_k[n]\beta_0}{\|\mathbf{D}_u[n]-\mathbf{D}_k\|^2+H^2} + \sum\limits_{i\in\mathcal{K}_O[n]}\frac{\alpha_i[n][m]\tilde{P}_i[n]\beta_0}{\|\mathbf{D}_u[n]-\mathbf{D}_i\|^2+H^2} + \sigma^2}{\sum\limits_{i\in\mathcal{K}_O[n]}\frac{\alpha_i[n][m]\tilde{P}_i[n]\beta_0}{\|\mathbf{D}_u[n]-\mathbf{D}_i\|^2+H^2} + \sigma^2}\right), \quad (41)$$

$$\hat{R}_k^I[n][m] = W\log_2\left(\sum_{i\in\mathcal{K}_O[n]}\frac{\alpha_i[n][m]\tilde{P}_i[n]\beta_0}{\|\mathbf{D}_u[n]-\mathbf{D}_i\|^2+H^2} + \sigma^2\right). \quad (42)$$

(39a) can be rewritten as

$$\rho[n] \leqslant T_n \cdot \sum_{k=1}^{K}\sum_{m=1}^{M}\left(-W\log_2\left(\sum_{i\in\mathcal{K}_O[n]}\frac{\alpha_i[n][m]\tilde{P}_i[n]\beta_0}{\|\mathbf{D}_u[n]-\mathbf{D}_i\|^2+H^2} + \sigma^2\right) + \bar{R}_k^I[n][m] + R_k^O[n][m]\right), \quad \forall n \in \mathcal{N}. \quad (43)$$

Referring to [23], we introduce the relaxation variable $\mathbf{S}$.

$$\mathbf{S} = \left\{s_{u,i}[n] = \|\mathbf{D}_u[n] - \mathbf{D}_i\|^2, \forall i \in \mathcal{K}_O[n], \forall n \in \mathcal{N}\right\}. \quad (44)$$

Therefore (39) can be written as

$$\max_{\mathbf{D}_u[n],\mathbf{S},\rho[n]} \ \rho[n]$$
$$s.t.\ \rho[n] \leqslant T_n \cdot \sum_{k=1}^{K}\sum_{m=1}^{M}\left(-W\log_2\left(\sum_{i\in\mathcal{K}_O[n]}\frac{\alpha_i[n][m]\tilde{P}_i[n]\beta_0}{s_{u,i}[n]+H^2} + \sigma^2\right) + \bar{R}_k^I[n][m] + R_k^O[n][m]\right), \quad \forall n \in \mathcal{N}, \quad (45a)$$
$$\|\mathbf{D}_u[n] - \mathbf{D}_i\|^2 \geqslant s_{u,i}[n], \ \forall i \in \mathcal{K}_O[n], \quad \forall n \in \mathcal{N}, \quad (45b)$$
$$\|\mathbf{D}_u[n+1] - \mathbf{D}_u[n]\|^2 \leqslant (V_{max} \cdot T_n)^2, \quad \forall n \in \mathcal{N}, \quad (45c)$$

$$\|\mathbf{D}_u[n]-\mathbf{D}_u[n-1]\|^2 \leqslant (V_{max}\cdot T_n)^2, \quad \forall n\in\mathcal{N}, \tag{45d}$$

$$\mathbf{D}_u[1]=\mathbf{D}_u[N+1]. \tag{45e}$$

It can be proved that (45b) holds with equality when problem (45) is optimal. Otherwise, we can always increase $s_{u,i}[n]$ without decreasing $\rho[n]$. (45a) is a non-convex set, because $\bar{R}_k^I[n][m]$ and $R_k^O[n][m]$ are non-concave function with respect to $\mathbf{D}_u[n]$. (45b) is a non-convex set because the superlevel set of the convex quadratic function is generally not a convex set. Therefore, (45) is a non-convex problem.

SCA can be used to deal with the non-convexity of (45a) by relaxing $\bar{R}_k^I[n][m]$ and $R_k^O[n][m]$ to concave function. Specifically, in each iteration, we perform the first-order Taylor expansion of $\bar{R}_k^I[n][m]$ and $R_k^O[n][m]$ at certain point $\mathbf{D}_u^{(r)}[n]$. Thus, (45a) is transformed into a convex set. The key to the transformation is that $\bar{R}_k^I[n][m]$ and $R_k^O[n][m]$ are convex function with respect to $\|\mathbf{D}_u[n]-\mathbf{D}_k\|^2$. According to [42], the first-order Taylor expansion of the convex function at any point is the global lower bound of the function. Therefore, this transformation does not expand the feasible region of problem (45).

Specifically, $\bar{R}_k^I[n][m]$ can be transformed to

$$\begin{aligned}
&\bar{R}_k^I[n][m]\\
&= W\log_2\left(\frac{\alpha_k[n][m]\tilde{P}_k[n]\beta_0}{\|\mathbf{D}_u[n]-\mathbf{D}_k\|^2+H^2}+\sum_{i\in\mathcal{K}_O[n]}\frac{\alpha_i[n][m]\tilde{P}_i[n]\beta_0}{\|\mathbf{D}_u[n]-\mathbf{D}_i\|^2+H^2}+\sigma^2\right)\\
&\geqslant -B_k^{I(r)}[n][m]\left(\begin{array}{c}\|\mathbf{D}_u[n]-\mathbf{D}_k\|^2-\\ \left\|\mathbf{D}_u^{(r)}[n]-\mathbf{D}_k\right\|^2\end{array}\right)+C_k^{I(r)}[n][m]\\
&\triangleq \bar{R}_k^{I(lb)}[n][m],
\end{aligned} \tag{46}$$

where

$$\begin{aligned}
&B_k^{I(r)}[n][m]\\
&= W\cdot\log_2(e)\\
&\cdot\left(\frac{\frac{\alpha_k[n][m]\tilde{P}_k[n]\beta_0}{\left(\left\|\mathbf{D}_u^{(r)}[n]-\mathbf{D}_k\right\|^2+H^2\right)^2}+\sum_{i\in\mathcal{K}_O[n]}\frac{\alpha_i[n][m]\tilde{P}_i[n]\beta_0}{\left(\left\|\mathbf{D}_u^{(r)}[n]-\mathbf{D}_i\right\|^2+H^2\right)^2}}{\frac{\alpha_k[n][m]\tilde{P}_k[n]\beta_0}{\left\|\mathbf{D}_u^{(r)}[n]-\mathbf{D}_k\right\|^2+H^2}+\sum_{i\in\mathcal{K}_O[n]}\frac{\alpha_i[n][m]\tilde{P}_i[n]\beta_0}{\left\|\mathbf{D}_u^{(r)}[n]-\mathbf{D}_i\right\|^2+H^2}+\sigma^2}\right),
\end{aligned} \tag{47}$$

$$\begin{aligned}
&C_k^{I(r)}[n][m]\\
&= W\cdot\log_2\left(\frac{\alpha_k[n][m]\tilde{P}_k[n]\beta_0}{\left\|\mathbf{D}_u^{(r)}[n]-\mathbf{D}_k\right\|^2+H^2}+\sum_{i\in\mathcal{K}_O[n]}\frac{\alpha_i[n][m]\tilde{P}_i[n]\beta_0}{\left\|\mathbf{D}_u^{(r)}[n]-\mathbf{D}_i\right\|^2+H^2}+\sigma^2\right).
\end{aligned} \tag{48}$$

$R_k^O[n][m]$ can be transformed to

$$\begin{aligned}
&R_k^O[n][m]\\
&= W\log_2\left(1+\frac{\alpha_k[n][m]\tilde{P}_k[n]\beta_0}{\sigma^2\left(\|\mathbf{D}_u[n]-\mathbf{D}_k\|^2+H^2\right)}\right)\\
&\geqslant -J_k^{I(r)}[n][m]\left(\begin{array}{c}\|\mathbf{D}_u[n]-\mathbf{D}_k\|^2-\\ \left\|\mathbf{D}_u^{(r)}[n]-\mathbf{D}_k\right\|^2\end{array}\right)+K_k^{I(r)}[n][m]\\
&\triangleq R_k^{O(lb)}[n][m],
\end{aligned} \tag{49}$$

where

$$\begin{aligned}
&J_k^{I(r)}[n][m]\\
&= W\cdot\frac{\log_2(e)\frac{\alpha_k[n][m]\tilde{P}_k[n]\beta_0}{\sigma^2\left(\left\|\mathbf{D}_u^{(r)}[n]-\mathbf{D}_k\right\|^2+H^2\right)^2}}{\log_2\left(1+\frac{\alpha_k[n][m]\tilde{P}_k[n]\beta_0}{\sigma^2\left(\left\|\mathbf{D}_u^{(r)}[n]-\mathbf{D}_k\right\|^2+H^2\right)}\right)},
\end{aligned} \tag{50}$$

$$\begin{aligned}
&K_k^{I(r)}[n][m]\\
&= W\cdot\log_2\left(1+\frac{\alpha_k[n][m]\tilde{P}_k[n]\beta_0}{\sigma^2\left(\left\|\mathbf{D}_u^{(r)}[n]-\mathbf{D}_k\right\|^2+H^2\right)}\right)
\end{aligned} \tag{51}$$

In the same way, because $\|\mathbf{D}_u[n]-\mathbf{D}_i\|_2^2$ is a convex function about $\mathbf{D}_u[n]$, we can perform the first-order Taylor expansion of $\|\mathbf{D}_u[n]-\mathbf{D}_i\|_2^2$ at certain point $\mathbf{D}_u^{(r)}[n]$ without expanding the set of constraint (45b).

$$\begin{aligned}
\|\mathbf{D}_u[n]-\mathbf{D}_i\|^2 \geqslant &\left\|\mathbf{D}_u^{(r)}[n]-\mathbf{D}_i\right\|^2+2\left(\mathbf{D}_u^{(r)}[n]-\mathbf{D}_i\right)^T\\
&\times\left(\mathbf{D}_u[n]-\mathbf{D}_u^{(r)}[n]\right),\ \forall i\in\mathcal{K}_O[n],\forall n\in\mathcal{N}.
\end{aligned} \tag{52}$$

Therefore, problem (45) can be rewritten as

$$\max_{\mathbf{D}_u[n],\mathbf{S},\rho[n]}\ \rho[n]$$

$$s.t.\ \ \rho[n]\leqslant T_n$$

$$\cdot\sum_{k=1}^{K}\sum_{m=1}^{M}\left(\begin{array}{c}\bar{R}_k^{I(lb)}[n][m]+R_k^{O(lb)}[n][m]\\ -W\log_2\left(\sum_{i\in\mathcal{K}_O[n]}\frac{\alpha_i[n][m]\tilde{P}_i[n]\beta_0}{s_{u,i}[n]+H^2}+\sigma^2\right)\end{array}\right),\quad \forall n\in\mathcal{N}, \tag{53a}$$

$$\left\|\mathbf{D}_u^{(r)}[n]-\mathbf{D}_i\right\|^2+2\left(\mathbf{D}_u^{(r)}[n]-\mathbf{D}_i\right)^T\times\left(\mathbf{D}_u[n]-\mathbf{D}_u^{(r)}[n]\right)\geqslant s_{u,i}[n],\quad \forall i\in\mathcal{K}_O[n],\ \forall n\in\mathcal{N}, \tag{53b}$$

$$\|\mathbf{D}_u[n+1]-\mathbf{D}_u[n]\|^2\leqslant(V_{max}\cdot T_n)^2,\quad \forall n\in\mathcal{N}, \tag{53c}$$

$$\|\mathbf{D}_u[n]-\mathbf{D}_u[n-1]\|^2\leqslant(V_{max}\cdot T_n)^2,\quad \forall n\in\mathcal{N}, \tag{53d}$$

$$\mathbf{D}_u[1]=\mathbf{D}_u[N+1]. \tag{53e}$$

Problem (53) is a convex optimization problem, which can be solved with CVX [42]. Due to the function relaxation, the optimal solution of problem (53) is the lower bound of the optimal solution of problem **P2**. And the optimal UAV trajectory of problem (53) can be denoted as $\hat{\mathbf{D}}_u[n]$.

The Algorithm 4 for problem **P2** is presented as follows.

Algorithm 4 Successive Convex Approximation Algorithm for Solving **P2**

Input: $\alpha_k^*[n][m]$, $\tilde{P}_k[n]$, the threshold ψ.
Output: Optimal $\hat{\mathbf{D}}_u[n]$, $\rho^*[n]$.

```
Set r = 1. Choose the initial UAV trajectory as D_u^(1)[n].
Calculate ρ^(1)[n].
repeat
    Obtain (46), (49) and (52) with given D_u^(r)[n], and add them to problem (53).
    Solve (53) with CVX, and get the optimal D̂_u[n].
    r ← r + 1, D_u^(r)[n] = D̂_u[n].
    Calculate ρ^(r)[n].
until |ρ^(r+1)[n] − ρ^(r)[n]| ⩽ ψ.
D̂_u[n] = D_u^(r)[n], ρ*[n] = ρ^(r)[n].
```

D. IoTD TRANSMIT POWER OPTIMIZATION

As shown in Figure 2, $R_1[n]$ represents the amount of uploaded data in time slot n, with given $\alpha_k^*[n][m]$, $\tilde{P}_k[n][m]$ and $\tilde{\mathbf{D}}_u[n]$. $R_2[n]$ is the optimal solution of problem (53). $R_2[n] = \rho^*[n]$. If $R_2[n] > R_1[n]$, it means that we can optimize the total energy consumption of IoTDs by solving problem **P3** with given $\alpha_k^*[n][m]$ and $\hat{\mathbf{D}}_u[n]$.

$$P3: \min_{P_k[n]} T_n \cdot \sum_{n=1}^{N}\sum_{k=1}^{K}\sum_{m=1}^{M} \alpha_k^*[n][m] P_k[n]$$
$$s.t.\ 0 \leqslant P_k[n] \leqslant P_{max}, \quad \forall k \in \mathcal{K},\ \forall n \in \mathcal{N}, \tag{54a}$$
$$T_n \cdot \sum_{n=1}^{N}\sum_{m=1}^{M} \left(R_k^I[n][m] + R_k^O[n][m]\right) \geqslant C_k, \quad \forall k \in \mathcal{K}. \tag{54b}$$

Problem **P3** is similar to problem (15), so Algorithm 2 can be applied to solve it. The optimal IoTD transmit power of problem (54) is denoted as $\hat{P}_k[n]$.

In summary, data collection optimization algorithm shown in Figure 2 is shown in **Algorithm** 5.

E. DESIGN OF GREEDY ALGORITHM

In order to reduce algorithm complexity, we propose a greedy algorithm for the NOMA-aided UAV data collection system. As shown in Algorithm 6, we propose an IoTD pairing scheme based on the amount of uploaded data and channel gain of IoTDs to optimize IoTD scheduling, and the initial UAV position is taken as the optimal UAV trajectory. In addition, more than two IoTDs are allowed to reuse the same channel in the same time slot in the greedy algorithm.

Algorithm 5 Data Collection Optimization Algorithm (DCOA) for Solving **P**

Input: $T, N, M, K, C_k, \mathbf{D}_k, P_{max}, \tau$.
Output: $\alpha_k^*[n][m]$, $P_k^*[n]$, $\mathbf{D}_u^*[n]$.

```
Initialize UAV trajectory according to (12), and get D_u[n].
Solve P1 with given D_u[n] by Algorithm 3, and get α_k^*[n][m], P̃_k[n], and E_1.
Set E_2 = 0.
repeat
    Calculate R_1[n] with given α_k^*[n][m], P̃_k[n] and D̃_u[n].
    Solve P2 with given α_k^*[n][m] and P̃_k[n] by Algorithm 4. Get D̂_u[n] and R_2[n].
    if R_2[n] > R_1[n] then
        Solve P3 with given α_k^*[n][m] and D̂_u[n], and get P̂_k[n] and E_2.
    else
        return P_k^*[n] = P̃_k[n], D_u^*[n] = D̃_u[n], E^* = E_1.
    end if
    if E_2 < E_1 then
        E_1 ← E_2, D̃_u[n] ← D̂_u[n], P̃_k[n] ← P̂_k[n].
    else
        P_k^*[n] = P̃_k[n], D_u^*[n] = D̃_u[n], E^* = E_1.
    end if
until E_2 > E_1 and |E_2 − E_1| < τ.
```

F. COMPUTATIONAL COMPLEXITY ANALYSIS

The computational complexity of the proposed algorithm DCOA and GA is analyzed as follows. The computational complexity of DCOA depends on Algorithm 2, 3 and 4. In the worst case, the computational complexity of Algorithm 2 is roughly estimated as $\mathcal{O}\left(u_{\max} r_{\max} K^2 M N^2\right)$. The primal problem of Algorithm 3 is solved by Algorithm 2. The master problem of Algorithm 3 is solved by the branch and bound method or the cut plane method, so its computational complexity is $\mathcal{O}\left((4KMN)^3\right)$ [44], [46]. In the worst case, the computational complexity of Algorithm 3 is roughly estimated as $\mathcal{O}\left(64 v_{\max} (KMN)^3\right)$. The computational complexity of Algorithm 4 in the worst case is roughly estimated as $\mathcal{O}\left(\max\left\{3 r_{\max} KMN^2, 8 r_{\max} N^4\right\}\right)$ [42]. Assume that the loop number of Algorithm 2 and Algorithm 4 in DCOA is L. The computational complexity of DCOA algorithm in the worst case is roughly estimated as (55). The GA algorithm consists of the following three parts: UAV trajectory optimization, IoTD scheduling and power optimization. The computational complexity of the three parts are roughly estimated as $\mathcal{O}(N)$, $\mathcal{O}\left(2K^3\right)$ and $\mathcal{O}\left(u_{\max} r_{\max} K^2 M N^2\right)$ respectively. Therefore, the computational complexity of the proposed GA algorithm in the worst case is roughly estimated as $\mathcal{O}\left(\max\left\{2K^3, u_{\max} r_{\max} K^2 M N^2\right\}\right)$.

$$\mathcal{O}\left(\max\left\{\begin{matrix} u_{\max} r_{\max} L K^2 M N^2, \\ 64 v_{\max} (KMN)^3, 8 r_{\max} L N^4 \end{matrix}\right\}\right). \tag{55}$$

Algorithm 6 Greedy Algorithm (GA) for NOMA-Aided UAV Data Collection System

Input: $T, N, M, K, C_k, \mathbf{D}_k, P_{max}$.
Output: $\alpha_k^*[n][m], P_k^*[n], \mathbf{D}_u^*[n]$.

1: Initialize UAV trajectory according to (12), and get $\mathbf{D}_u[n]$ and r_u. Initialize $\alpha_k[n][m] = 0$.
2: $\mathbf{D}_u^*[n] = \mathbf{D}_u[n]$.
3: Obtain $\mathcal{K}_I$ and $\mathcal{K}_O$ with given $\mathbf{D}_u^*[n]$, r_u and $\mathbf{D}_k$.
4: **for** $n = 1 : N$ **do**
5: Get $\tilde{\mathcal{K}}_I[n]$ by sequencing IoTDs in $\mathcal{K}_I[n]$ from large to small according to C_k.
6: **repeat**
7: Assign channel for IoTDs in $\tilde{\mathcal{K}}_I[n]$ according to their sequence number.
8: For $k \in \tilde{\mathcal{K}}_I[n]$, $\alpha_k[n][m] = 1$. M is the sequence number of IoTD k.
9: **until** $m > M$ **or** All IoTDs in $\tilde{\mathcal{K}}_I[n]$ are assigned.
10: **end for**
11: $\mathcal{K}_Y = \mathcal{K} \backslash \mathcal{K}_I$.
12: Get $\tilde{\mathcal{K}}_Y$ by sequencing IoTDs in $\mathcal{K}_Y$ from large to small according to C_k.
13: **repeat**
14: Assign channel for IoTDs in $\tilde{\mathcal{K}}_Y$ according to their sequence number.
15: For $k \in \tilde{\mathcal{K}}_Y$, $\alpha_k[n][m] = 1$. IoTD k is closest to UAV in time slot n. m is the channel number of idle channel in time slot n.
16: **until** All channels are assigned.
17: **repeat**
18: Let $P_k = P_{max}$. According to (6) and (7), calculate $\tilde{C}_k = T_n \cdot \sum_{n=1}^{N} \sum_{m=1}^{M} R_k[n][m]$.
19: $\hat{C}_k = C_k - \tilde{C}_k$.
20: **if** $\hat{C}_k > 0$ **then**
21: Let $k \in \mathcal{K}_Y$. $C_k = \hat{C}_k$.
22: **else**
23: Let $k \in \mathcal{K}_N$.
24: **end if**
25: Get $\tilde{\mathcal{K}}_Y$ by sequencing IoTDs in $\mathcal{K}_Y$ from large to small according to C_k.
26: Get $\tilde{\mathcal{K}}_N$ by sequencing IoTDs in $\mathcal{K}_N$ from small to large according to C_k.
27: Assign channel according to the sequence number of IoTD k in $\tilde{\mathcal{K}}_Y$.
28: For $k \in \tilde{\mathcal{K}}_Y$, $\alpha_k[n][m] = 1$. The time slot n and the channel number m are the same as those of IoTD j ($j \in \tilde{\mathcal{K}}_N$), and the sequence number of IoTD j in step 26 is same as the sequence number of IoTD k in step 25.
29: **until** $\mathcal{K}_Y = \emptyset$.
30: **return** $\alpha_k^*[n][m] = \alpha_k[n][m]$.
31: Calculate optimal $P_k^*[n]$ with given $\alpha_k^*[n][m]$, $\mathbf{D}_u^*[n]$ according to **Algorithm 2**.

IV. NUMERICAL RESULTS

In this section, numerical results are presented to demonstrate the performance of the proposed algorithm. In the simulation, we assume that IoTDs are randomly distributed in a circular area with radius $R = 70$ m. The amount of uploaded data C_k varies randomly from 1 Mbit to 5 Mbit. The maximum transmit power is $P_{max} = 4$ W. The flight height and maximum flight speed of UAV are $H = 50$ m and $V_{max} = 7$ m/s. The trajectory initialization parameter is set as $\varsigma = 0.7$. Furthermore, assuming the number of system channels is $M = 7$ and the bandwidth of sub-channel is $W = 30$ kHz. The normalized channel gain is $\beta_0 = -50$ dB. The noise power is $\sigma^2 = -100$ dBm.

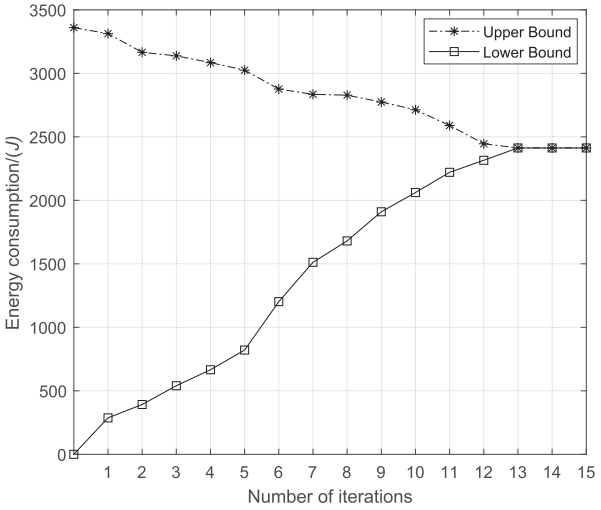

FIGURE 3. Convergence of GBD algorithm.

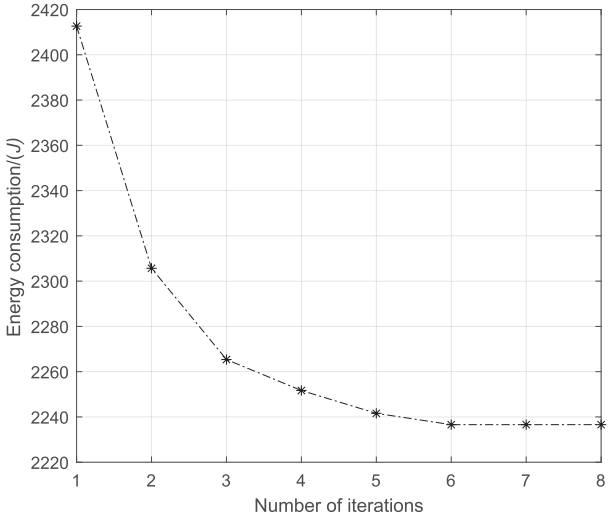

FIGURE 4. Convergence of the two-step iteration optimization algorithm.

In Figure 3 and Figure 4, we evaluate the convergence performance of GBD algorithm and the two-step iterative optimization algorithm for problems **P2** and **P3** in DCOA. We set $N = 6$, $K = 70$ and $T = 60s$. As shown in Figure 3, for GBD algorithm, the initial upper bound is set to the maximum energy consumption of IoTDs ($2 \cdot 6 \cdot 7 \cdot 10s \cdot$

4W = 3360 J), and the lower bound is 0 J. It can be found that the difference between the upper bound and the lower bound gradually decreases and GBD algorithm converges after 13 iterations. For the two-step iterative optimization algorithm shown in Figure 4, the initial value is the total energy consumption optimized by GBD algorithm, and it converges after 6 iterations. It can be seen that the minimum energy consumption can be obtained with several iterations in DCOA, which shows that DCOA is effective.

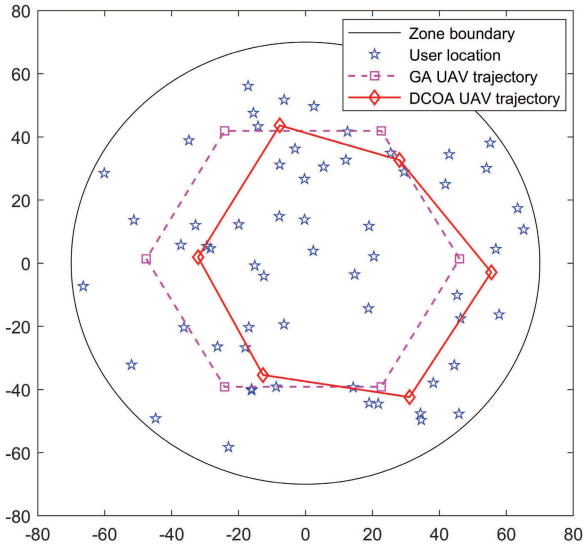

FIGURE 5. The distribution of IoTDs and optimized UAV trajectory.

Figure 5 shows the distribution of IoTDs and UAV trajectory optimized by GA and DCOA, respectively, when $N = 6$, $K = 60$ and $T = 60s$. The GA UAV trajectory is the initial UAV trajectory according to (12), and the DCOA UAV trajectory is the UAV trajectory optimized by DCOA algorithm. In this paper, the GA UAV trajectory is designed based on the amount of uploaded data and the location of IoTDs, with the goal of ensuring IoTDs fairness. Moreover, it can be observed that the DCOA UAV trajectory is around the GA UAV trajectory. This is due to the fact that the DCOA UAV trajectory is optimized based on the GA UAV trajectory. Because the increase in the channel gain difference of IoTDs which access the same channel in NOMA is conducive to the reduction of energy consumption. In order to minimize the total energy consumption of IoTDs, UAV tends to be close to IoTDs with large amount of uploaded data and away from IoTDs with small amount.

In Figure 6, we compare the total energy consumption of IoTDs achieved by GA algorithm and DCOA algorithm under different numbers of IoTDs when $N = 6$ and $T = 60\text{s}, 70\text{s}, 80\text{s}$. It can be observed that the total energy consumption presents an exponential growth with the increase in the number of IoTDs. This is because that the power domain NOMA scheme is realized at the cost of increasing of IoTDs power. In addition, in terms of NOMA,

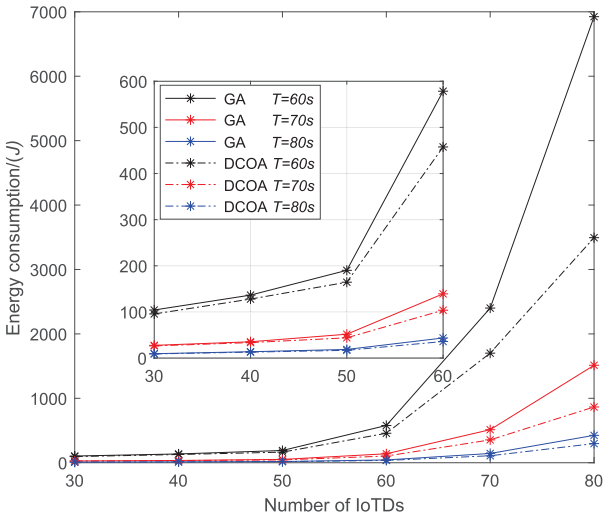

FIGURE 6. Total energy consumption versus the number of IoTDs parameterized by different UAV flight time.

interference from co-channel IoTDs is much greater than noise. Thus, according to equations (6) and (7), the power of internal IoTD needs to be increased several times to ensure the data rate. Therefore, when the number of IoTDs is less than the number of channels ($K = 30, 40$), IoTDs are more likely to upload data by OMA to reduce energy consumption. As the number of IoTDs increases ($K = 60, 70, 80$), the number of NOMA IoTDs increases, resulting in the exponential growth of IoTDs energy consumption.

In addition, compared with GA algorithm, DCOA algorithm can effectively reduce the total energy consumption when $K = 60, 70, 80$. The more IoTDs, the more obvious the advantages of DCOA. The reason is that the pairing of IoTDs can affect the transmit power of IoTDs greatly, and DCOA algorithm optimizes IoTD scheduling by GBD algorithm. And the distance between UAV and paired IoTDs is optimized to reduce the interference from external IoTD by optimizing UAV trajectory.

Note: When $K = 80$, we set $P_{max} = 10$W to get a generalized simulation result, which can intuitively show the impact of the increased number of IoTDs on the total energy consumption.

Figure 7 shows the total energy consumption versus UAV flight time optimized by DCOA algorithm and GA algorithm when $N = 6$, $K = 60, 70, 80$ and $r_u = 23.3958$m. It can be observed that the total energy consumption decreases exponentially with UAV flight time increasing. The reason is as follows. First, according to constraint (9b), $P \propto \sqrt[T_n]{2^c}$ and $c = C_k/W$. So, IoTD transmit power decreases rapidly with the increase of flight time, especially when T_n or c is large. Second, when the power of external IoTDs decreases, its interference with internal IoTDs also decreases, according to equation (6), which can significantly reduce the power of the internal IoTDs. Therefore, as presented in Figure 7, although communication time increases linearly, the total

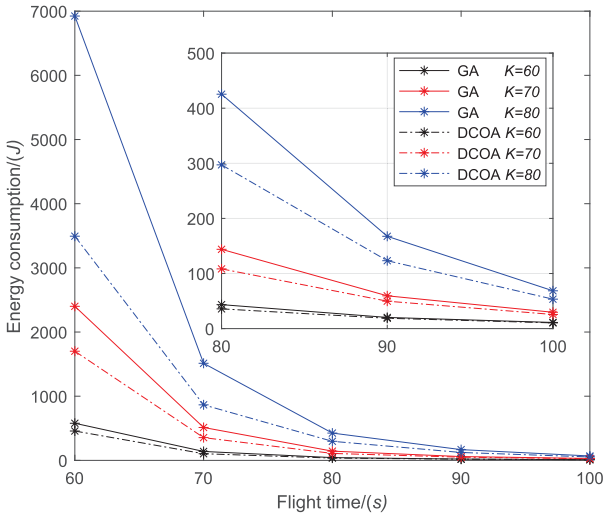

FIGURE 7. Total energy consumption versus UAV flight time parameterized by the number of IoTDs.

energy consumption of IoTDs decreases exponentially. From the numerical results, it can be found that increasing UAV flight time will greatly improve the performance of the proposed NOMA-aided UAV data collection system in terms of the total energy consumption of IoTDs.

In fact, UAV flight time is generally unchangeable, but T_n can be changed with the value of N. Therefore, in Figure 8, we analyze the impact of N on total energy consumption.

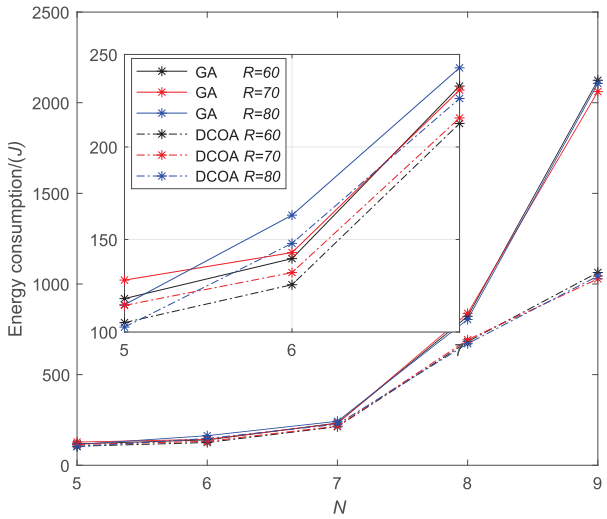

FIGURE 8. Total energy consumption versus the value of N.

In Figure 8, we simulate the total energy consumption optimized by DCOA algorithm and GA algorithm when $K = 60$, $T = 70$s and $R = 60$m, 70m, 80m. It can be observed that with unchangeable UAV flight time, the total energy consumption increases significantly as N increases. Therefore, combining with the results of Figure 7, we can conclude as follows. For the proposed NOMA-aided UAV data collection system, in terms of reducing total energy consumption of IoTDs, reducing N to increase the length of one time slot T_n is more effective than increasing N to increase the number of subchannels. In addition, as shown in Figure 8, small change of the radius R has little effect on the total energy consumption.

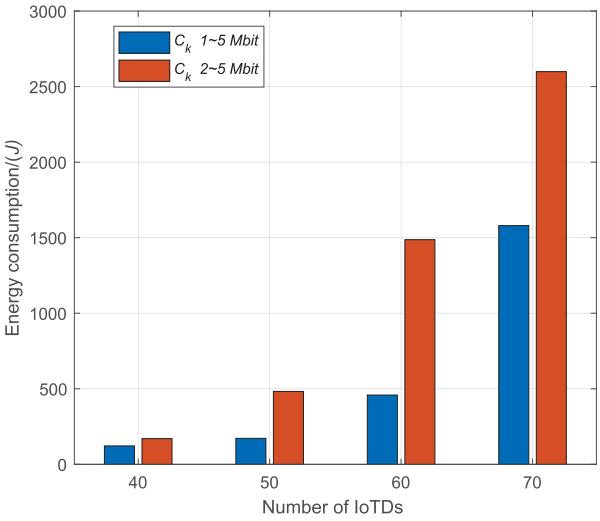

FIGURE 9. Total energy consumption versus the amount of IoTDs uploaded data C_k.

In Figure 9, we analyze the impact of the amount of IoTD uploaded data on the total energy consumption optimized by DCOA algorithm. We set $N = 6$, $T = 60$s and the number of IoTD uploaded data is 1 Mbit $\sim$ 5 Mbit or 2 Mbit $\sim$ 5 Mbit. It can be observed that when the number of IoTD is large, the range of data volume of IoTDs will greatly affect the total energy consumption. And the larger the range of data volume changes, the lower the total energy consumption. Therefore, based on numerical results, we can find that the proposed UAV-aided NOMA data collection system is suitable for collecting data in inaccessible areas where multiple IoTDs with large differences in data volume coexist.

TABLE 1. Runtime of GA and DCOA.

The number of IoTDs	$K = 40$	$K = 50$	$K = 60$
GA runtime	17.322 s	21.135 s	27.688 s
DCOA runtime	153.430 s	181.672 s	209.625 s

Furthermore, we compare the runtime of GA algorithm and DCOA algorithm under the same computer configuration when $N = 6$, $R = 70$m and $T = 60$s. As shown in Table 1, the runtime of GA algorithm is greatly shortened since the optimization of UAV trajectory and IoTD scheduling is simplified. Combining the results of Figure 6 and Figure 7, compared with DCOA algorithm, the performance of GA algorithm decreases little when the number of IoTDs is small or UAV flight time is long. Therefore, in the above situation, GA algorithm may be more advantageous.

Finally, we compare the impact of NOMA and OMA on the success rate of data collection when $T = 70$s. For NOMA, we set $N = 6$. For OMA, in order to ensure the access of IoTDs, the number of subchannels should be more than the

number of IoTDs. So, we set $N = 8$ when $K = 50$ and $N = 9$ when $K = 60$. As shown in Table 2, NOMA technology is more suitable than OMA technology for collecting data within limited time.

TABLE 2. Success rate of IoTDs uploading data.

The number of IoTDs	$K = 50$	$K = 60$
OMA	97.040%	93.683%
NOMA	100%	100%

V. CONCLUSION

In this paper, we have investigated a NOMA-aided UAV communication system to collect data within UAV flight time for large-scale IoTDs in inaccessible areas. Specifically, UAV trajectory, IoTD scheduling and transmit power are jointly optimized to minimize the total energy consumption of IoTDs while ensuring data collection. Then data collection optimization algorithm is proposed to get the sub-optimal solution relying on the Generalized Benders Decomposition and successive convex approximation techniques. And we propose the greedy algorithm to reduce complexity by simplifying the optimization of UAV trajectory and IoTD scheduling. Finally, the numerical results demonstrate that, compared with the traditional UAV communication systems, the proposed NOMA-aided UAV system performs better in terms of the data collection and DCOA can effectively reduce the total energy consumption of IoTDs.

APPENDIX A
SOLUTION OF THE FEASIBILITY CUT

The calculation of $\tilde{\boldsymbol{\eta}}^{(v)}$ and $\tilde{P}_k[n]$ can be achieved by solving the following $\ell_1 \sim norm$ problem when the primal problem is infeasible.

$$\min_{s_k, P_k[n]} \sum_{k=1}^{K} s_k$$
$$s.t.\ 0 \leqslant P_k[n] \leqslant P_{max}, \quad \forall k \in \mathcal{K},\ \forall n \in \mathcal{N}, \tag{56a}$$
$$C_k - T \cdot \sum_{n=1}^{N}\sum_{m=1}^{M}\left(R_k^I[n][m] + R_k^O[n][m]\right) \leqslant s_k, \quad \forall k \in \mathcal{K}. \tag{56b}$$

Similar to (23)-(27), (55b) can be transformed into

$$\hat{G}\left(P_k[n]\right) \leqslant s_k, \tag{57}$$

where

$$\begin{aligned} G\left(P_k[n]\right) &= C_k - T \cdot \sum_{n=1}^{N}\sum_{m=1}^{M}\left(R_k^I[n][m] + R_k^O[n][m]\right) \\ &\leqslant C_k - T \cdot \sum_{n=1}^{N}\sum_{m=1}^{M}\left(\bar{R}_k^I[n][m] - \hat{R}_k^{I(up)}[n][m] \right. \\ &\quad \left. + R_k^O[n][m]\right) \\ &= \hat{G}\left(P_k[n]\right) \end{aligned} \tag{58}$$

Thus, problem (56) can be transformed into a convex problem. The optimal solution $\tilde{P}_k[n]$ and $\tilde{\boldsymbol{\eta}}$ satisfy the following KKT conditions.

$$\begin{aligned} 1 - \sum_{k=1}^{K} \tilde{\eta}_k &= 0 \\ \sum_{k=1}^{K} \tilde{\eta}_k \cdot \nabla_{P_k[n]} \hat{G}(\tilde{P}_k[n]) &= 0 \\ \tilde{\eta}_k \cdot \left[\hat{G}_k(\tilde{P}_k[n]) - s_k\right] &= 0 \\ \tilde{\eta}_k &\geqslant 0 \end{aligned} \tag{59}$$

Therefore, if the primal problem is infeasible in the v-th iteration of GBD, the optimal solution $\tilde{P}_k^{(v)}[n]$ and $\tilde{\boldsymbol{\eta}}^{(v)}$ can be obtained by (59). Then we can get the feasibility cut as follows.

$$\begin{aligned} &\bar{\mathfrak{L}}(\alpha_k[n][m], \tilde{P}_k^{(v)}[n], \tilde{\boldsymbol{\eta}}^{(v)}) \\ &= \sum_{k=1}^{K} \tilde{\eta}_k^{(v)} \left(C_k - T \cdot \sum_{n=1}^{N}\sum_{m=1}^{M}\left(R_k^I[n][m] + R_k^O[n][m]\right)\right) \leqslant 0 \end{aligned} \tag{60}$$

REFERENCES

[1] L. Chettri and R. Bera, "A comprehensive survey on Internet of Things (IoT) toward 5G wireless systems," *IEEE Internet Things J.*, vol. 7, no. 1, pp. 16–32, Jan. 2020.
[2] M. F. Elrawy, A. I. Awad, and H. F. A. Hamed, "Intrusion detection systems for IoT-based smart environments: A survey," *J. Cloud Comput.*, vol. 7, no. 1, pp. 1–21, Dec. 2018.
[3] O. Elijah, T. A. Rahman, I. Orikumhi, C. Y. Leow, and M. H. D. N. Hindia, "An overview of Internet of Things (IoT) and data analytics in agriculture: Benefits and challenges," *IEEE Internet Things J.*, vol. 5, no. 5, pp. 3758–3773, Oct. 2018.
[4] P. Verma and S. K. Sood, "Fog assisted-IoT enabled patient health monitoring in smart homes," *IEEE Internet Things J.*, vol. 5, no. 3, pp. 1789–1796, Jun. 2018.
[5] Cisco. *Internet of Things*. Accessed: Feb. 2020. [Online]. Available: https://emarsonindia.com/wp-content/uploads/2020/02/Internet-of-Things.pdf
[6] Y.-P.-E. Wang, X. Lin, A. Adhikary, A. Grovlen, Y. Sui, Y. Blankenship, J. Bergman, and H. S. Razaghi, "A primer on 3GPP narrowband Internet of Things," *IEEE Commun. Mag.*, vol. 55, no. 3, pp. 117–123, Mar. 2017.
[7] H.-C. Lee and K.-H. Ke, "Monitoring of large-area IoT sensors using a LoRa wireless mesh network system: Design and evaluation," *IEEE Trans. Instrum. Meas.*, vol. 67, no. 9, pp. 2177–2187, Sep. 2018.
[8] B. Li, Z. Fei, and Y. Zhang, "UAV communications for 5G and beyond: Recent advances and future trends," *IEEE Internet Things J.*, vol. 6, no. 2, pp. 2241–2263, Apr. 2019.
[9] Da-Jiang Innovations. *Technical Parameters of UAV*. Accessed: May 2020. [Online]. Available: https://www.dji.com/cn
[10] L. Dai, B. Wang, Z. Ding, Z. Wang, S. Chen, and L. Hanzo, "A survey of non-orthogonal multiple access for 5G," *IEEE Commun. Surveys Tuts.*, vol. 20, no. 3, pp. 2294–2323, 3rd Quart., 2018.
[11] A. Al-Hourani, S. Kandeepan, and A. Jamalipour, "Modeling air-to-ground path loss for low altitude platforms in urban environments," in *Proc. IEEE Global Commun. Conf.*, Dec. 2014, pp. 2898–2904.
[12] D. W. Matolak and R. Sun, "Air–ground channel characterization for unmanned aircraft systems—Part III: The suburban and near-urban environments," *IEEE Trans. Veh. Technol.*, vol. 66, no. 8, pp. 6607–6618, Jan. 2017.
[13] R. Sun and D. W. Matolak, "Air–Ground channel characterization for unmanned aircraft systems part II: Hilly and mountainous settings," *IEEE Trans. Veh. Technol.*, vol. 66, no. 3, pp. 1913–1925, Mar. 2017.
[14] D. Yang, Q. Wu, Y. Zeng, and R. Zhang, "Energy tradeoff in ground-to-UAV communication via trajectory design," *IEEE Trans. Veh. Technol.*, vol. 67, no. 7, pp. 6721–6726, Jul. 2018.

[15] H. Wu, X. Tao, N. Zhang, and X. Shen, "Cooperative UAV cluster-assisted terrestrial cellular networks for ubiquitous coverage," *IEEE J. Sel. Areas Commun.*, vol. 36, no. 9, pp. 2045–2058, Sep. 2018.
[16] A. A. Khuwaja, Y. Chen, and G. Zheng, "Effect of user mobility and channel fading on the outage performance of UAV communications," *IEEE Wireless Commun. Lett.*, vol. 9, no. 3, pp. 367–370, Mar. 2020.
[17] J. Chakareski, S. Naqvi, N. Mastronarde, J. Xu, F. Afghah, and A. Razi, "An energy efficient framework for UAV-assisted millimeter wave 5G heterogeneous cellular networks," *IEEE Trans. Green Commun. Netw.*, vol. 3, no. 1, pp. 37–44, Mar. 2019.
[18] Y. Zeng, J. Xu, and R. Zhang, "Energy minimization for wireless communication with rotary-wing UAV," *IEEE Trans. Wireless Commun.*, vol. 18, no. 4, pp. 2329–2345, Apr. 2019.
[19] Y. Sun, D. Xu, D. W. K. Ng, L. Dai, and R. Schober, "Optimal 3D-trajectory design and resource allocation for solar-powered UAV communication systems," *IEEE Trans. Commun.*, vol. 67, no. 6, pp. 4281–4298, Jun. 2019.
[20] C. Zhan, Y. Zeng, and R. Zhang, "Energy-efficient data collection in UAV enabled wireless sensor network," *IEEE Wireless Commun. Lett.*, vol. 7, no. 3, pp. 328–331, Jun. 2018.
[21] M. Mozaffari, W. Saad, M. Bennis, and M. Debbah, "Mobile unmanned aerial vehicles (UAVs) for energy-efficient Internet of Things communications," *IEEE Trans. Wireless Commun.*, vol. 16, no. 11, pp. 7574–7589, Nov. 2017.
[22] X. Lin, G. Su, B. Chen, H. Wang, and M. Dai, "Striking a balance between system throughput and energy efficiency for UAV-IoT systems," *IEEE Internet Things J.*, vol. 6, no. 6, pp. 10519–10533, Dec. 2019.
[23] Q. Wu, Y. Zeng, and R. Zhang, "Joint trajectory and communication design for multi-UAV enabled wireless networks," *IEEE Trans. Wireless Commun.*, vol. 17, no. 3, pp. 2109–2121, Mar. 2018.
[24] Y. Saito, Y. Kishiyama, A. Benjebbour, T. Nakamura, A. Li, and K. Higuchi, "Non-orthogonal multiple access (NOMA) for cellular future radio access," in *Proc. IEEE 77th Veh. Technol. Conf. (VTC Spring)*, Jun. 2013, pp. 1–5.
[25] Y. Saito, A. Benjebbour, Y. Kishiyama, and T. Nakamura, "System-level performance evaluation of downlink non-orthogonal multiple access (NOMA)," in *Proc. IEEE 24th Annu. Int. Symp. Pers., Indoor, Mobile Radio Commun. (PIMRC)*, Sep. 2013, pp. 611–615.
[26] X. Wang, J. Wang, L. He, and J. Song, "Outage analysis for downlink NOMA with statistical channel state information," *IEEE Wireless Commun. Lett.*, vol. 7, no. 2, pp. 142–145, Apr. 2018.
[27] Z. Ding, Z. Yang, P. Fan, and H. V. Poor, "On the performance of non-orthogonal multiple access in 5G systems with randomly deployed users," *IEEE Signal Process. Lett.*, vol. 21, no. 12, pp. 1501–1505, Dec. 2014.
[28] L. Zhu, J. Zhang, Z. Xiao, X. Cao, and D. O. Wu, "Optimal user pairing for downlink non-orthogonal multiple access (NOMA)," *IEEE Wireless Commun. Lett.*, vol. 8, no. 2, pp. 328–331, Apr. 2019.
[29] M. A. Sedaghat and R. R. Muller, "On user pairing in uplink NOMA," *IEEE Trans. Wireless Commun.*, vol. 17, no. 5, pp. 3474–3486, May 2018.
[30] F. Fang, J. Cheng, and Z. Ding, "Joint energy efficient subchannel and power optimization for a downlink NOMA heterogeneous network," *IEEE Trans. Veh. Technol.*, vol. 68, no. 2, pp. 1351–1364, Feb. 2019.
[31] M. Zeng, N.-P. Nguyen, O. A. Dobre, Z. Ding, and H. V. Poor, "Spectral- and energy-efficient resource allocation for multi-carrier uplink NOMA systems," *IEEE Trans. Veh. Technol.*, vol. 68, no. 9, pp. 9293–9296, Sep. 2019.
[32] M. Pischella and D. Le Ruyet, "NOMA-relevant clustering and resource allocation for proportional fair uplink communications," *IEEE Wireless Commun. Lett.*, vol. 8, no. 3, pp. 873–876, Jun. 2019.
[33] T. Hou, Y. Liu, Z. Song, X. Sun, and Y. Chen, "Multiple antenna aided NOMA in UAV networks: A stochastic geometry approach," *IEEE Trans. Commun.*, vol. 67, no. 2, pp. 1031–1044, Feb. 2019.
[34] T. Hou, Y. Liu, Z. Song, X. Sun, and Y. Chen, "Exploiting NOMA for UAV communications in large-scale cellular networks," *IEEE Trans. Commun.*, vol. 67, no. 10, pp. 6897–6911, Oct. 2019.
[35] M. F. Sohail, C. Y. Leow, and S. Won, "Energy-efficient non-orthogonal multiple access for UAV communication system," *IEEE Trans. Veh. Technol.*, vol. 68, no. 11, pp. 10834–10845, Nov. 2019.
[36] N. Zhao, X. Pang, Z. Li, Y. Chen, F. Li, Z. Ding, and M.-S. Alouini, "Joint trajectory and precoding optimization for UAV-assisted NOMA networks," *IEEE Trans. Commun.*, vol. 67, no. 5, pp. 3723–3735, May 2019.
[37] F. Cui, Y. Cai, Z. Qin, M. Zhao, and G. Y. Li, "Multiple access for mobile-UAV enabled networks: Joint trajectory design and resource allocation," *IEEE Trans. Commun.*, vol. 67, no. 7, pp. 4980–4994, Jul. 2019.
[38] R. Tang, J. Cheng, and Z. Cao, "Joint placement design, admission control, and power allocation for NOMA-based UAV systems," *IEEE Wireless Commun. Lett.*, vol. 9, no. 3, pp. 385–388, Mar. 2020.
[39] Y. Cai, Z. Wei, R. Li, D. W. K. Ng, and J. Yuan, "Joint trajectory and resource allocation design for energy-efficient secure UAV communication systems," *IEEE Trans. Commun.*, vol. 68, no. 7, pp. 4536–4553, Jul. 2020.
[40] A. M. Geoffrion, "Generalized benders decomposition," *J. Optim. Theory Appl.*, vol. 10, no. 4, pp. 237–260, Oct. 1972.
[41] M. J. Bagajewicz and V. Manousiouthakis, "On the generalized benders decomposition," *Comput. Chem. Eng.*, vol. 15, no. 10, pp. 691–700, Oct. 1991.
[42] S. Boyd, S. P. Boyd, and L. Vandenberghe, *Convex Optimization*. Cambridge, U.K.: Cambridge Univ. Press, 2004.
[43] R. Hemmecke, M. Köppe, J. Lee, and R. Weismantel, "Nonlinear integer programming," in *50 Years of Integer Programming 1958–2008*. Berlin, Germany: Springer, 2010, pp. 561–618.
[44] O. K. Gupta and A. Ravindran, "Branch and bound experiments in convex nonlinear integer programming," *Manage. Sci.*, vol. 31, no. 12, pp. 1533–1546, Dec. 1985.
[45] A. J. Conejo, E. Castillo, R. Minguez, and R. Garcia-Bertrand, *Decomposition Techniques in Mathematical Programming: Engineering and Science Applications*. New York, NY, USA: Springer, 2006.
[46] A. Basu, M. Conforti, M. Di Summa, and H. Jiang, "Complexity of cutting planes and branch-and-bound in mixed-integer optimization," 2020, *arXiv:2003.05023*. [Online]. Available: http://arxiv.org/abs/2003.05023

JUNWEI ZHAO received the B.S. degree in communications engineering from the Beijing University of Posts and Telecommunications, Beijing, China, in 2017, where he is currently pursuing the Ph.D. degree in telecommunication and information systems with the State Key Laboratory of Networking and Switching Technology. His research interests include UAV communication and radio resource management in future wireless networks.

YING WANG (Member, IEEE) received the Ph.D. degree in circuits and systems from the Beijing University of Posts and Telecommunications (BUPT), Beijing, China, in 2003. She was invited to work as a Visiting Researcher with the Communications Research Laboratory (renamed NiCT from 2004), Yokosuka, Japan, in 2004. She was a Research Associate with The University of Hong Kong, Hong Kong, in 2005. She is currently a Professor with BUPT and the Director of the Radio Resource Management Laboratory, Wireless Technology Innovation Institute, BUPT. She is active in standardization activities of 3GPP and ITU. She took part in performance evaluation work of the Chinese Evaluation Group, as a Representative of BUPT. She has authored over 100 papers in international journals and conferences proceedings. Her research interests include cooperative and cognitive systems, radio resource management, and mobility management in 5G systems. She was a recipient of first prizes of the Scientific and Technological Progress Award by the China Institute of Communications, in 2006 and 2009, respectively, and a second prize of the National Scientific and Technological Progress Award, in 2008. She was also selected in the New Star Program of Beijing Science and Technology Committee and the New Century Excellent Talents in University, Ministry of Education, in 2007 and 2009, respectively.

ZIXUAN FEI received the B.S. degree in communication engineering from Xidian University, Xi'an, Shaanxi, China, in 2015. He is currently pursuing the Ph.D. degree in information and communication engineering with the Beijing University of Posts and Telecommunications (BUPT), Beijing, China. His research interests include the multi-media IoT networks and resource management in fog computing.

XUE WANG received the B.S. degree in communication engineering from Jilin University, China, in 2018. She is currently pursuing the Ph.D. degree in information and communication engineering with the State Key Laboratory of Networking and Switching Technology, Beijing University of Posts and Telecommunications. Her research interests include smart grid, network slicing, and wireless resource management in future wireless networks.

ZHONGYU MIAO (Associate Member, IEEE) received the B.S. degree in communications engineering from the Beijing University of Posts and Telecommunications, Beijing, China, in 2014, where she is currently pursuing the Ph.D. degree in telecommunication and information systems with the Wireless Technology Innovation Institute. Her research interests include heterogeneous networks, cooperative communication, and physical layer security in future wireless networks.